CORROSION BEHAVIOR OF TITANIUM DIOXIDE (TiO_2)-COATED Al ALLOY IN SALINE ENVIRONMENT

By

MD Fazlay Rabbey, B.Sc.

A Project Submitted in Partial Fulfillment of the Requirements

for the Degree of

Master of Science

in

Mechanical Engineering

University of Alaska Fairbanks

August 2018

APPROVED:

Lei Zhang, Committee Chair
Junqing Zhang, Committee Member
Daisy Huang, Committee Member
Rorik Peterson, Committee Member
Rorik Peterson, Chair
Department of Mechanical Engineering

Abstract

Al alloys have been used in many applications, however, they are susceptible to corrosion when exposed in saline environment. In this work, TiO_2 nanoellipsoids with aspect ratios (AR) of 1, 2, 4 and 6 were synthesized, TiO_2 coatings of AR 1, AR2, AR4, and AR6 were fabricated on AA2024-T3 Al alloy substrate, and their corrosion behaviors in the saline environment were investigated by analyzing the scanning electron microscope (SEM) imaging, potentiodynamic polarization scans and electrochemical impedance spectroscopy. TiO_2-coated Al samples showed better corrosion performance compared to the bare Al sample. Among the coated samples, TiO_2 AR6 coated samples showed lower corrosion rate compared to other samples. Although TiO_2 nanoellipsoids coatings show good corrosion resistance, it is noted that TiO_2 coatings are porous, which allows the penetration of corrosive media through the pores to reach the surface of the substrate. A polystyrene (PS)-TiO_2 AR6 nanocomposite coating was fabricated, where the pores of the coatings were sealed by polystyrene, which is expected to further improve the corrosion resistance of TiO_2 coatings.

Table of Contents

List of Figures

List of Tables

Chapter 1

Introduction and Motivation

Aluminum alloys were introduced in the 1920s and since then drastic improvements have been made due to a better understanding of their chemical composition, impurity control, and the wide use of different heat treatments. Aluminum alloys are generally used in transportation, packaging, and construction. For example, aluminum and its alloys have been used as the primary materials for critical structures like frames and bodies of aircraft. In the late 1920s, aluminum alloys replaced wood and became the main airframe materials due to their light weight, high strength, and low cost. So far, 70% of aircraft airframe is made of aluminum alloys (measured by weight) [1].

Although Al alloys have been used in many applications, they are susceptible to corrosion when exposed in saline environment, where the combination of temperature, chemical and stress-related conditions can cause environmental cracking corrosion. This process can lead to stress corrosion cracking (SCC), corrosion fatigue, and hydrogen-induced cracking [2,3].

Many strategies have been used for corrosion mitigation and prevention. Environmental modification, surface treatment, cathodic protection, use of corrosion inhibitors, and application of coatings are the common methods. Among the methods, deposition of a coating on metallic alloys is one of the most commonly used methods because it is convenient and effective [2,4]. Before selecting a coating, many factors need to be considered such as the environment that the coating will be exposed, accessibility of the structure, operating temperature of the structure, cost, and surface preparation requirements etc. Before coating deposition, surface treatment of substrate is important. It is known that some premature failures are caused by inadequate and improper surface preparation of the substrate. Residues of oil, grease, soil, non-visible salts, rust

on the surface will weaken the adhesion of coating to substrate and accelerate the corrosion. Initial surface cleaning and preparation by cleaning and roughened surface for long-term stability is the key step to the success of the coating system. Therefore, surface blasting is required to clean the surface and creates an anchor profile to improve coating adhesion. A good coating should be tough and resilient enough to resist developing failed areas with time and to withstand reasonable stress, has good adhesion, easy to repair, and environmentally friendly. So far, a variety of coatings have been developed such as polymer coatings [5], oxide coatings [6], and composite coatings [7], among which chromate coatings have exhibited excellent corrosion resistance [8]. However, chromate coatings are toxic and their application has been limited. Therefore, it is imperative to develop new coatings which are effective and environmentally friendly.

TiO_2 coating has been used for corrosion prevention as it is effective, easy to produce, and environmentally friendly [9]. Shen et al. reported that TiO_2 nanoparticle coating provided the excellent corrosion protection on 316 L stainless steel. They showed the corrosion current density decreased by 3 orders of magnitude after applying TiO_2 coating on 316 L stainless steel, corrosion impedance increased by 100 times and corrosion potential shifted positively compared to the bare steel in the same environment. Currently, most studies are focused on the corrosion performance of TiO_2 coatings made of spherical particles; however, corrosion behavior of TiO_2 coatings of nanoellipsoids is unexplored. It is reported that TiO_2 nanoellipsoid coatings have shown excellent mechanical strength [4] and it is expected that TiO_2 nanoellipsoid coatings will exhibit good corrosion resistance.

In this work, TiO_2 nanoellipsoids with aspect ratios (AR) of 1, 2, 4 and 6 were synthesized, TiO_2 coatings of AR 1, AR2, AR4, and AR6 were fabricated on AA2024-T3 Al alloy substrate,

and their corrosion behaviors in the saline environment were investigated. Although TiO_2 nanoellipsoids coatings show good corrosion resistance, it is noted that TiO_2 coatings are porous, which allows the penetration of corrosive media through the pores to reach the surface of the substrate. It was reported that nanocomposites containing highly anisotropic nanoparticles with a small amount of polymer exhibit exceptional strength, stiffness and toughness [4, 10-15]. To further improve the corrosion resistance of TiO_2 coatings, in this work, the pores of the coatings were sealed by a polymer, polystyrene (PS). A PS-TiO_2 AR6 nanocomposite coating was fabricated. Future work will be focused on investigating the corrosion behavior of PS-TiO_2 nanocomposite coatings.

Chapter 2

Materials and Methods

2.1 Synthesis of TiO_2 Nanoellipsoids

Titanium Dioxide (TiO_2) nanoellipsoids with different aspect ratios (AR) of 1, 2, 4 and 6 were synthesized by using a hydrothermal (gel-sol) method. A mixture of triethanolamine (TEOA), titanium (IV) isopropoxide (TIPO), deionized (DI) water and $NH_3 \cdot H_2O$ were kept in the oven for 24 hours at 100 °C, and the mixture was transferred into an autoclave and kept in the oven for another 72 hours at 130 °C. After taking out from oven, the product was washed using DI water and centrifuged four times to collect the particles. The particles were freeze-dried to get dry powder.

2.2 TiO_2 coating fabrication

To compare the corrosion properties of coatings made of TiO_2 nanoellipsoids with different aspect ratios, TiO_2 coatings with similar thicknesses of around 5 μm were made using a spin coating method. AA2024-T3 Al alloy sheet was cut into small pieces with the size of 10 mm × 10 mm × 1 mm. The Al alloy samples were then polished using SiC papers to increase the surface roughness for the subsequent coating process. The samples were ultrasonically cleaned by soaking in acetone in a water bath sonicator for 15 min, and then rinsed with deionized water and dried using an air nozzle to remove any organic matter. The samples were then plasma-treated to make the surface hydrophilic and improve surface adhesion properties. To make TiO_2 coatings, TiO_2 aqueous suspensions of AR1, AR2, AR4 and AR6 nanoellipsoids with concentrations of 52 wt%, 51 wt%, 44 wt% and 35 wt%, respectively, were made. TiO_2 suspensions were spin coated on the Al alloy substrate at a rotation speed of 2200, 2400, 2100 and 2000 rpm for 3 min for AR1, AR2, AR4 and AR6 coatings, respectively.

2.3 Characterization

Scanning electron microscope (SEM) images were taken using A JEOL JXA-8530F electron microprobe in the advanced instrumentation lab (AIL) at UAF to characterize the morphology of coatings. Samples before and after electrochemical testing were digitally photographed.

2.4 Corrosion Tests

Corrosion behavior of the bare and TiO_2-coated Al alloy samples in 3.5 wt% NaCl aqueous solution was evaluated at room temperature. Potentiodynamic polarization and electrochemical impedance spectroscopy (EIS) tests were employed to determine the optimum aspect ratio of the TiO_2 nanoellipsoids in the coatings in terms of anti-corrosion performance. These experiments were performed using a computer controlled Corrosion Cell Kit (Gamry Instruments, Inc.) in the materials lab at the department of mechanical engineering at UAF. The corrosion cell consists of a saturated calomel electrode reference electrode, a graphite counter electrode, and the coated sample with an exposed area of 0.7854 cm^2 as the working electrode. The polarization and EIS curves were collected after 10 min of exposure at open circuit potential once a day within 3-week immersion duration. The polarization curves were measured at a scanning rate of 3 mV/s and the EIS tests were carried out in a range of 0.1 Hz to 100 kHz with an AC voltage amplitude of 10 mV. All potentiodynamic polarization and EIS data were analyzed using the Gamry echem analyst software.

Chapter 3

Characterization of TiO_2 Coatings

3.1 Morphology of TiO_2 nanoellipsoids

SEM images in Figure 1 show the morphologies of the as-synthesized TiO_2 nanoellipsoids with aspect ratio of 1, 2, 4 and 6. The minor axis for AR1 particles was 2a = 24 ± 3 nm, the major axis was 2b = 31 ± 6 nm, AR = 1.31 ± 0.39; for AR2 particles: 2a = 28 ± 3 nm, 2b = 73 ± 10 nm, AR = 2.58 ± 0.52; for AR4 particles: 2a = 28 ± 4 nm, 2b = 134 ± 22 nm, AR = 4.75 ± 0.60; for AR6 particles: 2a = 32 ± 5 nm, 2b = 204 ± 33 nm, AR = 6.41 ± 1.33. This is consistent with the reported results [4]. It is noted that the size of TiO_2 nanoellipsoids with the same aspect ratio is very uniform with a small size distribution.

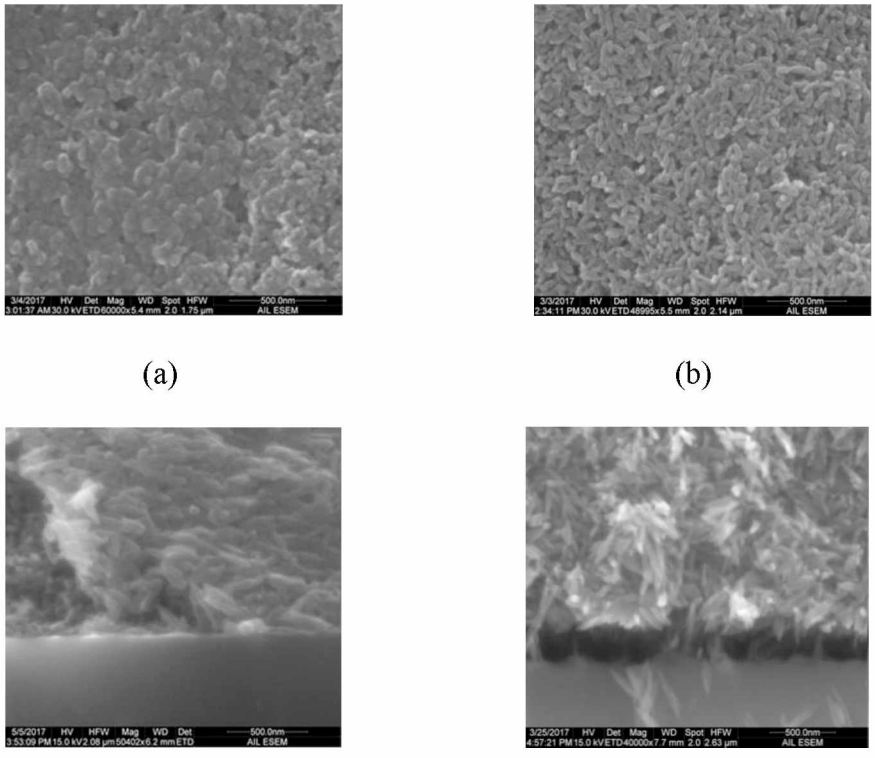

(a) (b)

(c) (d)

Figure 1: SEM images showing the morphologies of TiO_2 nanoellipsoids with an aspect ratio of (a) 1, (b) 2, (c) 4 and (d) 6.

3.2 TiO_2 coatings

TiO_2 coatings were made via spin coating method. It is known that spin-coated coating thickness is dependent on solution concentration and spin coating speed. In general, the higher the solution concentration and the lower the spin coating speed, the thicker the coating. To compare the corrosion properties of TiO_2 coatings made of ellipsoids with different ratios under the same conditions, coatings of TiO_2 AR1 to AR6 with similar thicknesses ranging from 4.6 to 5.7 μm were made by adjusting the solution concentration and spin coating speed. In [Table 1], it presents the spin coating parameters for TiO_2 coating fabrication. The solution concentrations for coatings of TiO_2 AR1, AR2, AR4, and AR6 were 50, 52, 44 and 35 wt%, respectively, and the spin coating speeds were 2200, 2400, 2100 and 2000, respectively.

Table 1: Spin coating parameters for TiO_2 coating fabrication.

TiO_2 (AR)	Solution Con. (wt%)	Spin Coater Speed (RPM)	Thickness (μm)
1	50	2200	5.7± 0.7
2	52	2400	4.6± 0.4
4	44	2100	4.6± 0.4
6	35	2000	5.0± 0.4

In the cross-section images (Figure 2) of TiO_2 coatings of AR 1 to AR 6, it can be seen that the coatings are very uniform and the thicknesses of all the coatings are around 5 μm (from 4.6 to 5.7 μm). This indicates that the as-fabricated TiO_2 coatings are of high quality, which will be subjected to corrosion tests in 3.5 wt% NaCl solution.

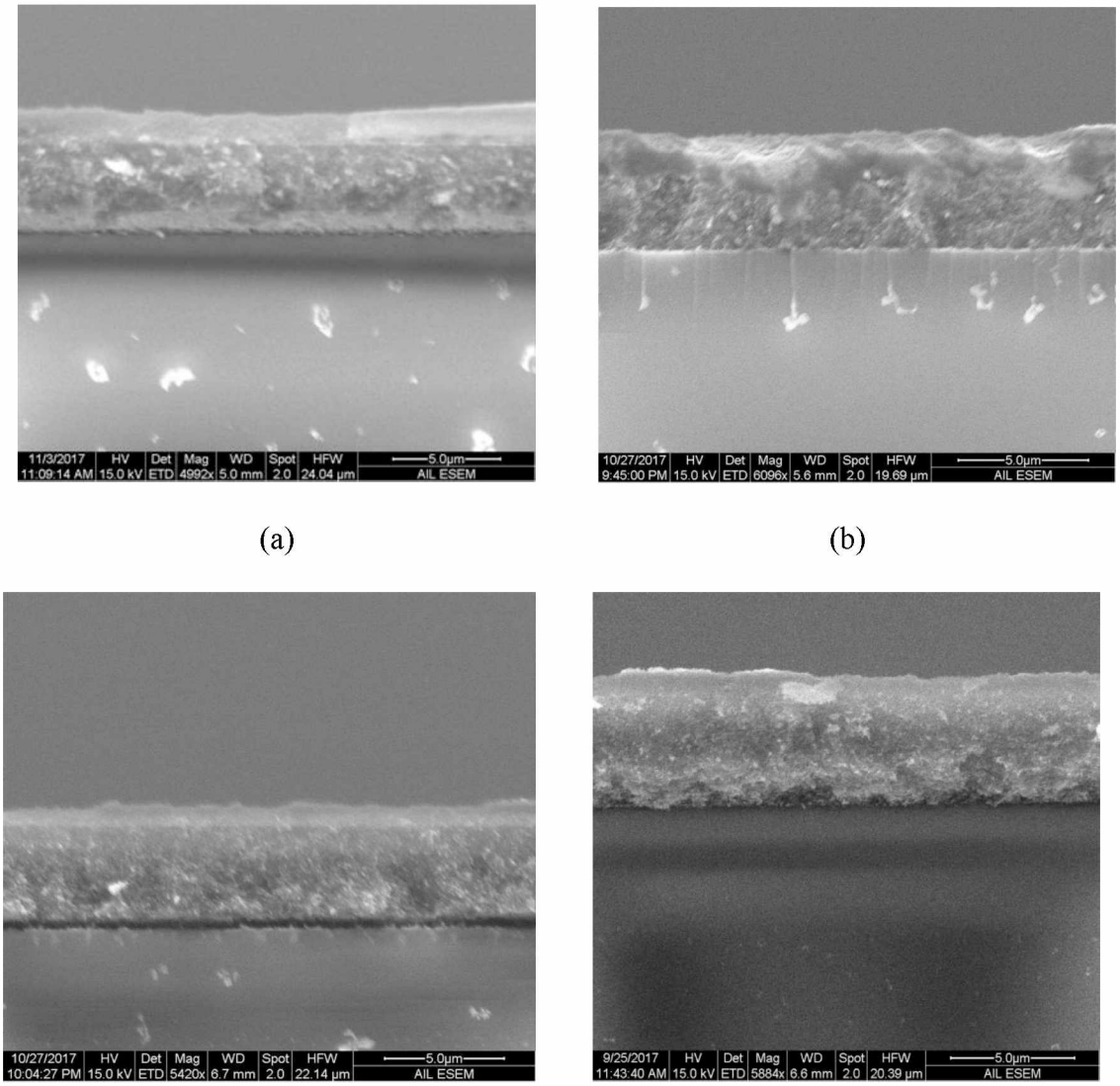

Figure 2: SEM cross-section images of TiO_2 coatings of (a) AR1, (b) AR2, (c) AR4 and (d) AR6.

Chapter 4

Corrosion Behavior of TiO_2-coated Al alloy in NaCl Solution

4.1 Macroscopic corrosion progression of bare and TiO_2-coated Al alloy samples

The macroscopic corrosion progression of TiO_2-coated and bare Al in 3.5wt% NaCl solution are shown in Figure 3. The sample surface was darkened after3-day immersion for bare Al, while other samples showed a light gray surface upon 7-day immersion. After 14-day immersion, bare Al sample showed a darker appearance and at 21-day immersion corrosion products can be observed on all the samples. Corrosion damage was observed for all samples except AR6 coating at 21-day immersion. The bare Al substrate was darkest and mostly deteriorated compared to other coated sample. This indicates that the TiO_2 coating is effective in corrosion protection of Al alloy. At 21-day immersion, all the TiO_2-coated samples except TiO_2 AR6-coated one showed obvious cracks, material loss, while TiO_2 AR6 coating showed very little material loss without obvious pitting.

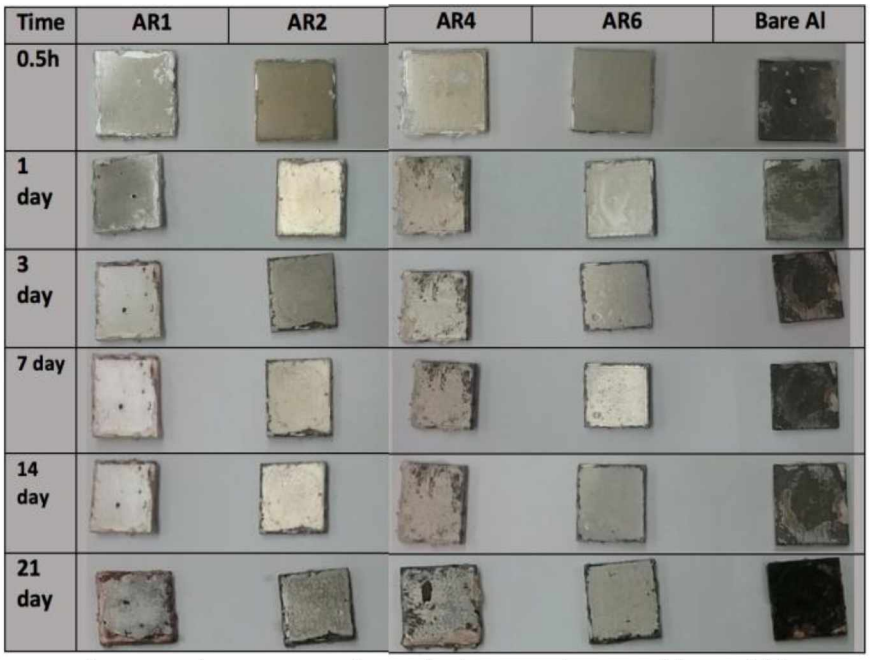

Figure 3: Macroscopic corrosion progression of TiO_2 coatings and bare Al in 3.5 wt% NaCl solution.

4.2 Potentiodynamic polarization of bare and TiO_2-coated Al alloy samples

Potentiodynamic polarization curves of bare Al and TiO_2-coated samples in 3.5wt% NaCl solution are shown in Figure 4. At 0.5-h immersion, the curve for the TiO_2 AR6 coating located leftmost among the other samples indicating the smallest current density. The curve for the bare Al substrate located rightmost for 1 day, 3 days, 7 days and 21 days, indicating a larger corrosion rate than the coated samples. The bare Al showed the highest negative potential while the coated samples positioned in the less negative direction. At early immersion time, samples showed lower current density, while at 14-day immersion, the samples showed higher current density. The corrosion potential values were typically less negative (more passive) for coated samples at early immersion time points and tended to be more negative with increasing immersion time. The bare Al showed a drop in corrosion current density following the 0.5 h immersion. This suggests the slower overall corrosion progression for the coated samples.

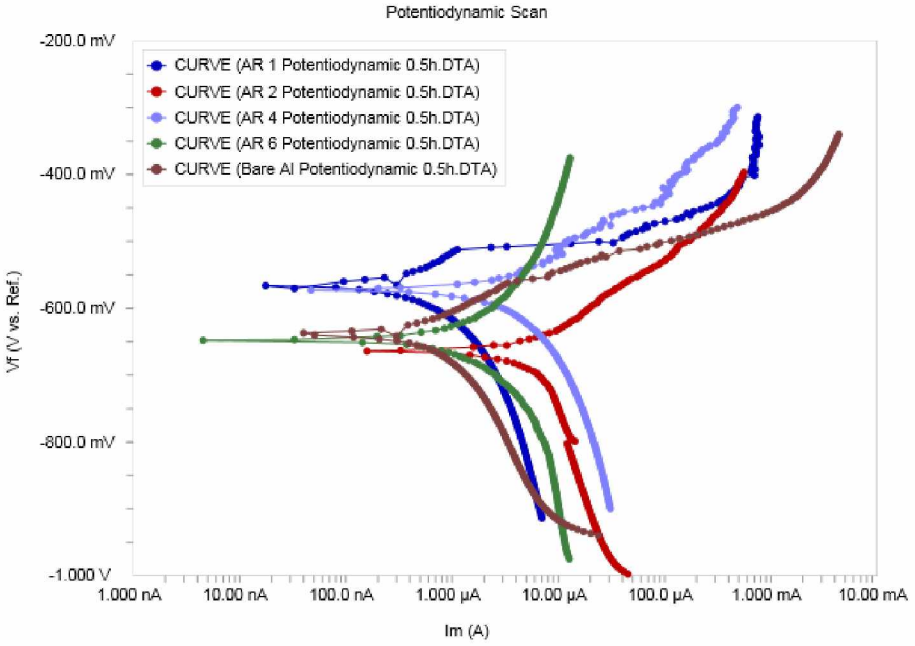

(a)

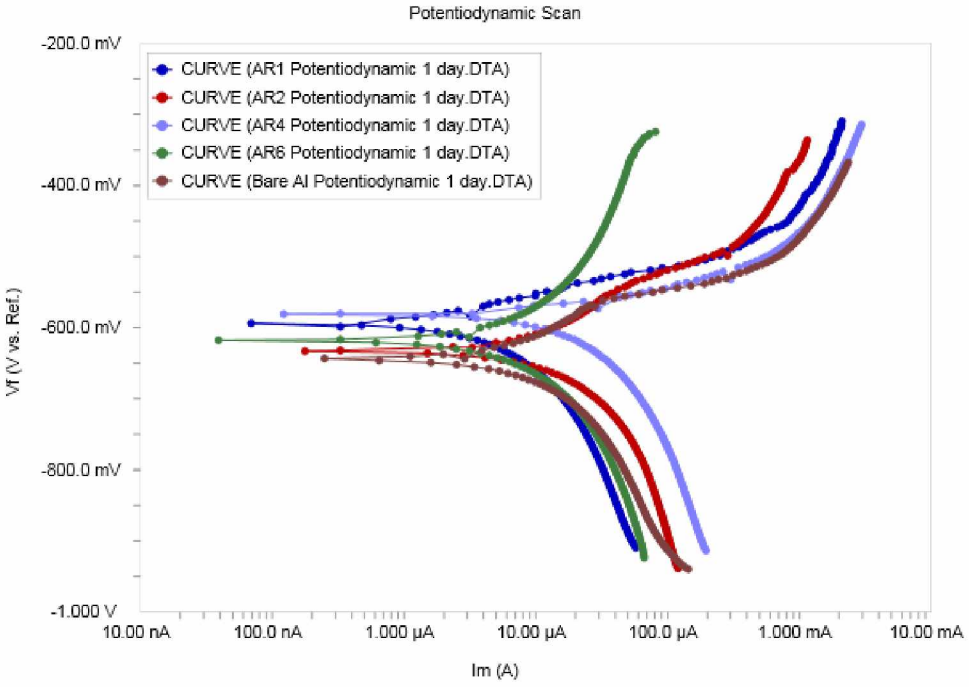
Potentiodynamic Scan
CURVE (AR1 Potentiodynamic 1 day.DTA)
CURVE (AR2 Potentiodynamic 1 day.DTA)
CURVE (AR4 Potentiodynamic 1 day.DTA)
CURVE (AR6 Potentiodynamic 1 day.DTA)
CURVE (Bare Al Potentiodynamic 1 day.DTA)
-200.0 mV
-400.0 mV
-600.0 mV
-800.0 mV
-1.000 V
Vf (V vs. Ref.)
10.00 nA
100.0 nA
1.000 µA
10.00 µA
100.0 µA
1.000 mA
10.00 mA
Im (A)

(b)

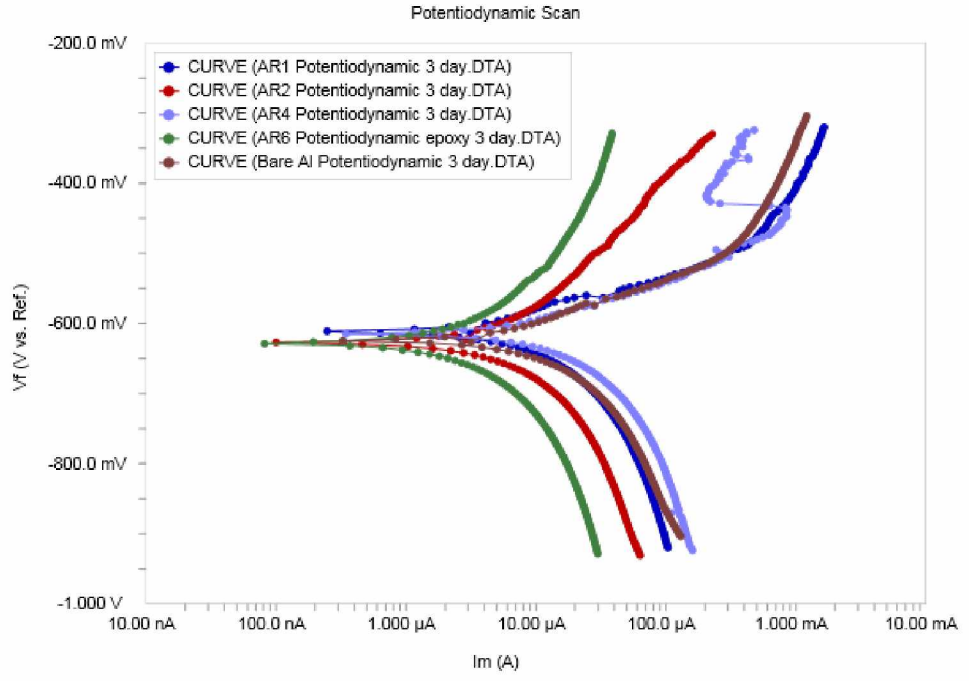
Potentiodynamic Scan
CURVE (AR1 Potentiodynamic 3 day.DTA)
CURVE (AR2 Potentiodynamic 3 day.DTA)
CURVE (AR4 Potentiodynamic 3 day.DTA)
CURVE (AR6 Potentiodynamic epoxy 3 day.DTA)
CURVE (Bare Al Potentiodynamic 3 day.DTA)
-200.0 mV
-400.0 mV
-600.0 mV
-800.0 mV
-1.000 V
Vf (V vs. Ref.)
10.00 nA
100.0 nA
1.000 µA
10.00 µA
100.0 µA
1.000 mA
10.00 mA
Im (A)

(c)

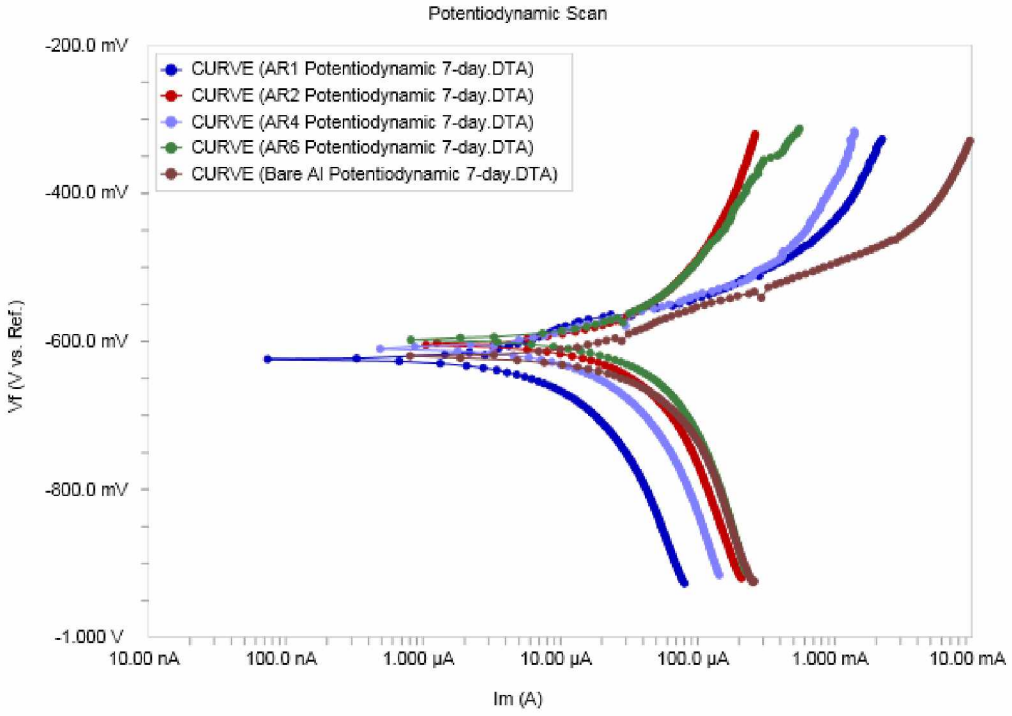
Potentiodynamic Scan
CURVE (AR1 Potentiodynamic 7-day.DTA)
CURVE (AR2 Potentiodynamic 7-day.DTA)
CURVE (AR4 Potentiodynamic 7-day.DTA)
CURVE (AR6 Potentiodynamic 7-day.DTA)
CURVE (Bare Al Potentiodynamic 7-day.DTA)
-200.0 mV
-400.0 mV
-600.0 mV
-800.0 mV
-1.000 V
Vf (V vs. Ref.)
10.00 nA
100.0 nA
1.000 µA
10.00 µA
100.0 µA
1.000 mA
10.00 mA
Im (A)

(d)

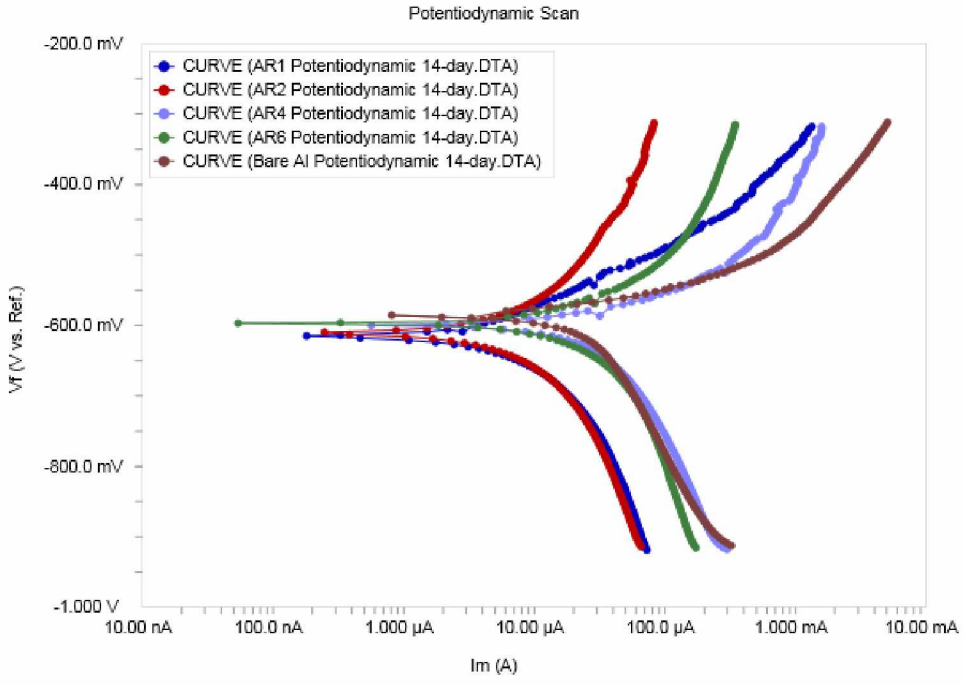
Potentiodynamic Scan
CURVE (AR1 Potentiodynamic 14-day.DTA)
CURVE (AR2 Potentiodynamic 14-day.DTA)
CURVE (AR4 Potentiodynamic 14-day.DTA)
CURVE (AR6 Potentiodynamic 14-day.DTA)
CURVE (Bare Al Potentiodynamic 14-day.DTA)
-200.0 mV
-400.0 mV
-600.0 mV
-800.0 mV
-1.000 V
Vf (V vs. Ref.)
10.00 nA
100.0 nA
1.000 µA
10.00 µA
100.0 µA
1.000 mA
10.00 mA
Im (A)

(e)

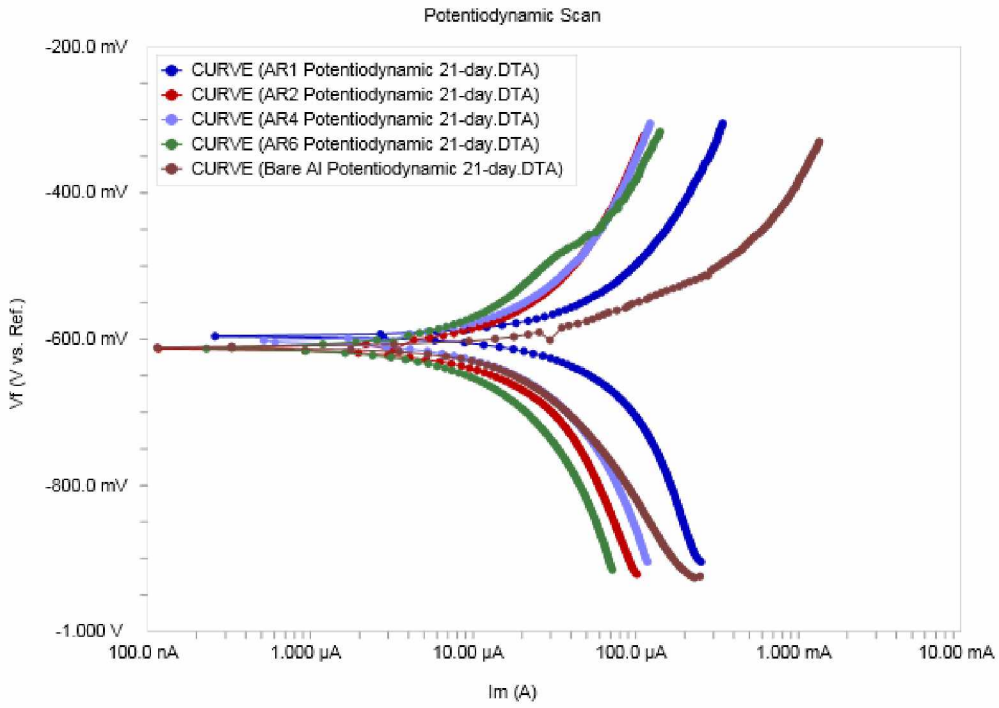

(f)

Figure 4: Potentiodynamic scans of TiO_2-coated and bare Al in 3.5wt% NaCl solution after (a) 0.5h (b) 1 day (c) 3 days (d) 7 days (e) 14 days and (f) 21 days

4.3 Electrochemical Impedance of bare and TiO_2-coated Al alloy samples

Figure 5 shows the electrochemical impedance of TiO_2 coatings and bare Al samples in the Bode plot. At 0.5-h immersion, the samples showed a trend of higher electrochemical impedance, whereas at 21-day immersion the samples showed decreased electrochemical impedance. Among the samples, the bare Al substrate had the lowest impedance regardless of immersion time and the AR6 coating had the highest electrochemical impedance, indicating the excellent corrosion resistance of TiO_2 AR6 coating. This result is consistent with the that of potentiodynamic polarization tests.

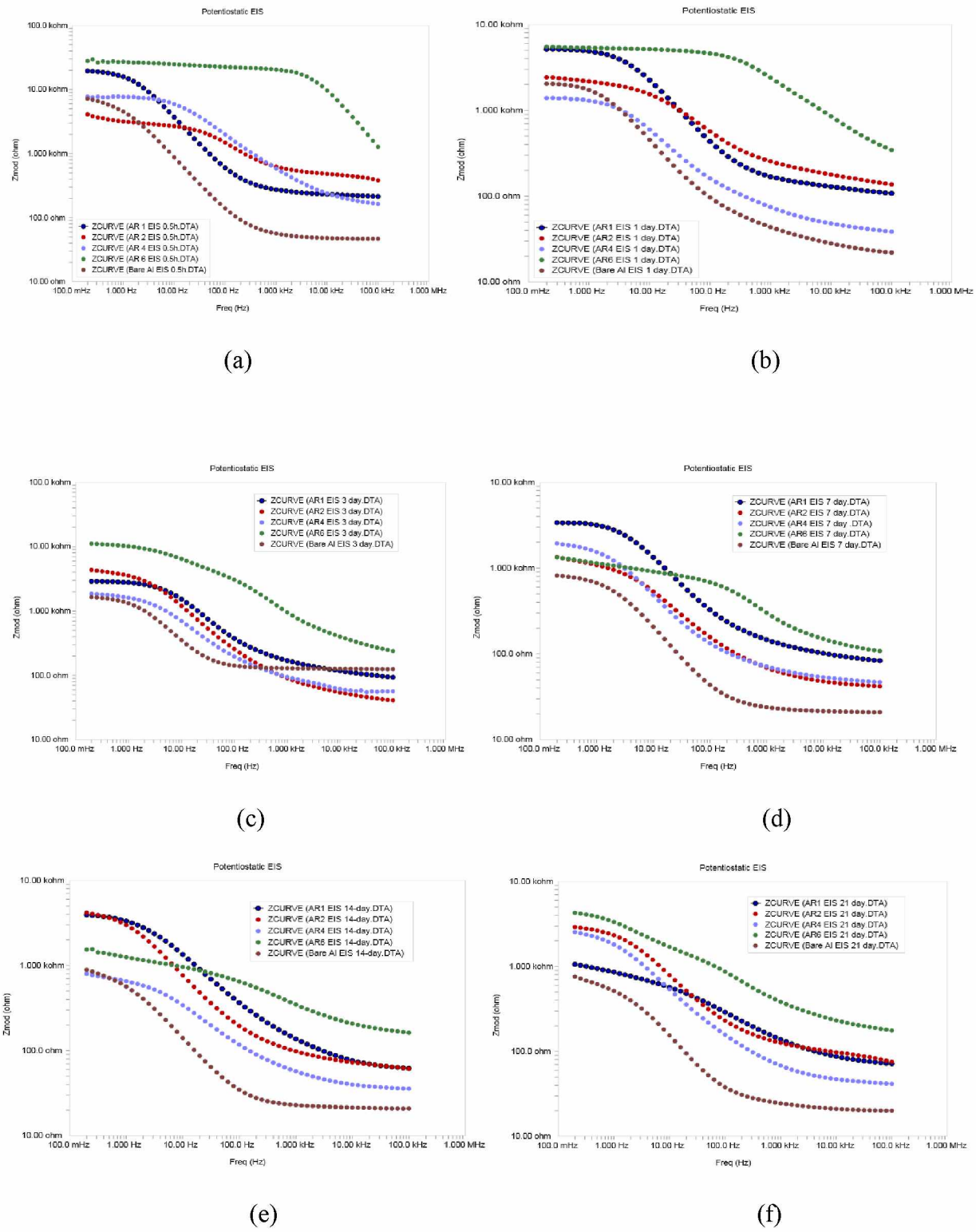

Figure 5: Electrochemical impedance of bare and TiO_2-coated Al samples after (a) 0.5 h (b) 1 day (c) 3 days (d) 7 days (e) 14 days and (f) 21 days

4.4 Corrosion potential (E_{corr}) and corrosion current density (I_{corr})

Table 2 shows the corrosion potential (E_{corr}) and corrosion current density (I_{corr}) of the samples evaluated by Tafel extrapolation at the linear stage of the anodic and cathodic curves. Extracted I_{corr} and E_{corr} values demonstrated a difference in the corrosion rates between the samples. The coated samples showed lower corrosion current density than the bare Al upon 14-day immersion, suggesting the lower corrosion rate of the coated samples. At 21-day immersion, the bare Al substrate showed a decrease in the current density, which may be due to the large amount of corrosion products formed on the surface acting as a barrier layer. When increasing the immersion time, generally the coated samples showed an increase in current density at around 7–21-day immersion due to the corrosion-generated defects and damage such as cracks and pitting holes. Among the coated samples, TiO_2 AR6 coated samples showed relatively lower corrosion current density compared to other samples, indicating their better corrosion performance.

Table 2: E_{corr} and I_{corr} values of bare and TiO_2-coated Al samples in 3.5 wt% NaCl solution determined by Tafel curve fit.

Samples	0.5 h		1-day		3-day		7-day		14-day		21-day	
	Icorr ($\mu A/cm^2$)	Ecorr (V)	Icorr ($\mu A/cm^2$)	Ecorr (V)	Icorr ($\mu A/cm^2$)	Ecorr (V)	Icorr ($\mu A/cm^2$)	Ecorr (V)	Icorr ($\mu A/cm^2$)	Ecorr (V)	Icorr ($\mu A/cm^2$)	Ecorr (V)
AR1	0.018	-0.566	0.069	−0.590	0.250	−0.610	0.074	−0.620	0.180	−0.610	0.260	-0.590
AR2	0.159	-0.664	0.180	−0.630	0.100	−0.630	1.050	−0.610	0.250	−0.610	0.120	−0.610
AR4	0.047	-0.570	0.120	−0.580	0.350	−0.610	0.490	−0.610	0.560	−0.600	0.520	−0.610
AR6	0.005	-0.648	0.038	-0.620	0.082	−0.630	0.815	−0.600	0.054	−0.590	0.230	−0.610
Bare Al	0.040	-0.637	0.250	−0.640	0.330	−0.630	0.800	−0.620	0.810	−0.590	0.114	−0.610

Chapter 5

Fabrication of Polymer-TiO_2 Nanocomposite Coatings (PTNC)

In Chapter 4, the results of corrosion tests show that TiO_2-coated Al alloy samples exhibited better corrosion resistance in saline environment. Since TiO_2 coatings are porous, it enables the penetration of corrosive media through the pores to reach the surface of substrate. To further improve the corrosion resistance of TiO_2 coatings, the pores of the coatings were sealed by a polymer, polystyrene (PS). A PS-TiO_2 nanocomposite coating was fabricated. In this chapter, preliminary results for the fabrication of PS-TiO_2 AR6 nanocomposite coating were discussed.

5.1 Fabrication of PTNC

AA2024-T3 Al alloy sheet was cut into small pieces with size of 10 mm × 10 mm × 1 mm. The Al alloy samples were then polished using SiC papers to increase the surface roughness for the subsequent coating process. The samples were ultrasonically cleaned by soaking in acetone in a water bath sonicator for 15 min, and then rinsed with deionized water and dried using an air nozzle to remove any organic matter. The samples were then plasma-treated to make the surface hydrophilic and improve surface adhesion properties. To fabricate the PTNC, a PS coating was first deposited on the plasma-treated Al alloy substrate using a spin coater followed by an oxygen plasma treatment again to make the surface of PS hydrophilic. TiO_2 AR6 coating was then spin coated on the plasma-treated PS layer at a rotational speed of 2000 rpm for 2 min to form a bilayer coating. The concentration of PS solution was 25 wt%, dissolved in toluene, and the concentration of TiO_2 AR6 aqueous solution was 35wt%. The bilayer coating was then annealed in an oven at 130 °C, until the pores in TiO_2 AR6 coating were completely filled with PS via capillary infiltration.

5.2 Characterization of PTNC

Figure 6 shows the process to make a polymer nanocomposite coating by capillary infiltration of polystyrene into the pores of TiO_2 AR6 coating. Figure 6a (5 μm scale) shows a bilayer coating consisting of PS and a TiO_2 AR6 coating before annealing. As shown in the image, the thickness of TiO_2 AR6 coating is about 5 μm and the PS coating is about 2.9 μm. The previous work reported that the porosity of TiO_2 AR6 coating is 58.4% [5]. To make polystyrene to be completely infiltrated into the pores of TiO_2 AR6 coating with a thickness of 5 μm, it was calculated that the thickness of PS layer should be at least 2.92 μm. To achieve this target value, spin coating speed was adjusted to control the PS coating thickness. The spin coating speeds and the corresponding PS coating thicknesses determined by SEM are shown in Table 3. The SEM images of the as-obtained PS coatings are shown in Figure 7. It shows that a thickness of about 2.9 μm can be achieved at a spin coating speed of 1560 rpm, which is close to the target thickness of 2.92 μm. Figure 6b (10 μm scale) shows the nanocomposite coating after the bilayer was annealed at 130 °C for 8 h. It can be seen that the PS coating disappeared, indicating that PS was completely infiltrated into TiO_2 AR6 coating after annealing, through which the pores of TiO_2 AR6 coating were effectively sealed. We expect that this PS-TiO_2 AR6 nanocomposite coating will show better corrosion performance than the TiO_2 AR6 coating. Future work will be focused on the fabrication of PS-TiO_2 nanocomposite coatings and investigation on their corrosion performance.

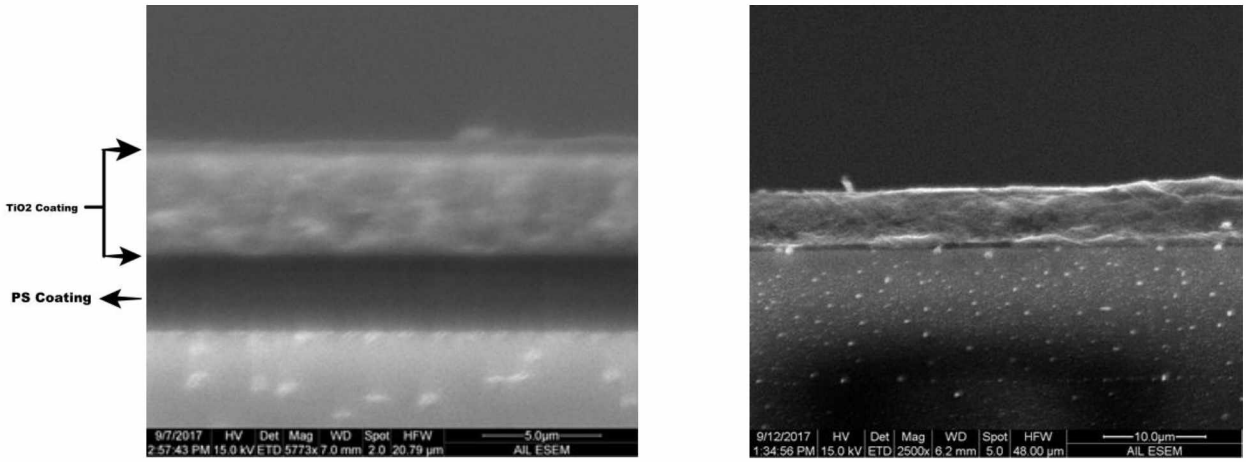

(a) (b)

Figure 6: SEM images showing capillary infiltration of a bilayer coating consisting of PS and a TiO_2 AR6 coating. From left to right, the SEM images are taken before and after the bilayer was annealed at 130 °C for 8 h.

Table 3: PS solution concentration, spin coating speed, and the as-obtained PS coating thicknesses

Polystyrene Solution Concentration (wt%)	Spin Coater Speed (RPM)	Thickness (µm)
25	2520	1.7 ± 0.05
25	2400	1.9 ± 0.05
25	2220	2.1 ± 0.10
25	1560	2.75 ± 0.20

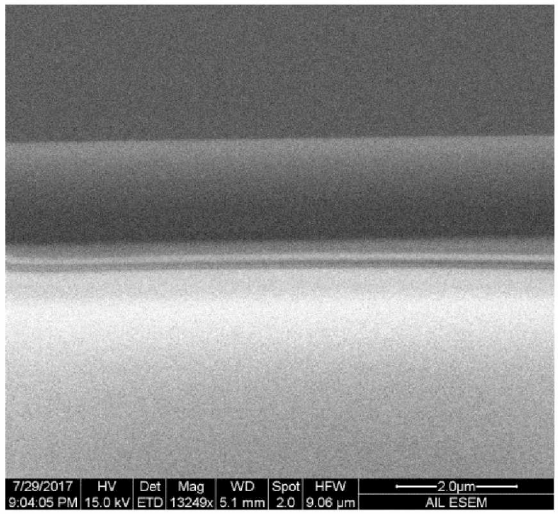

(a)

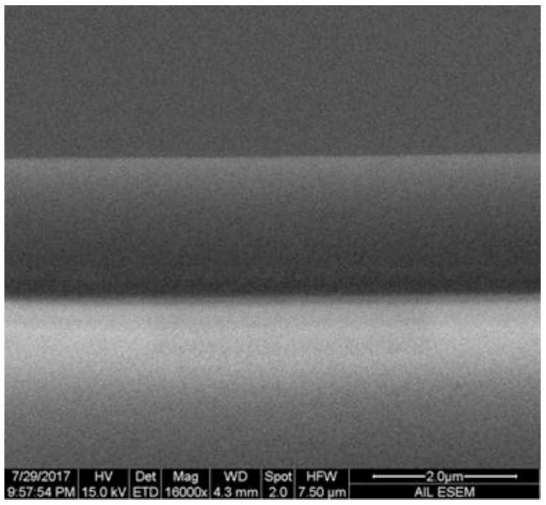

(b)

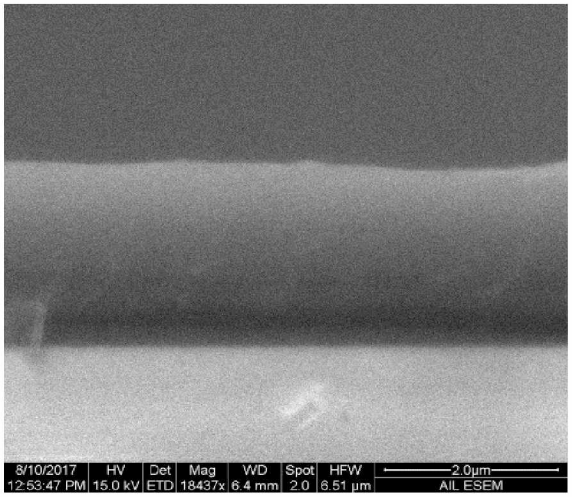

(c)

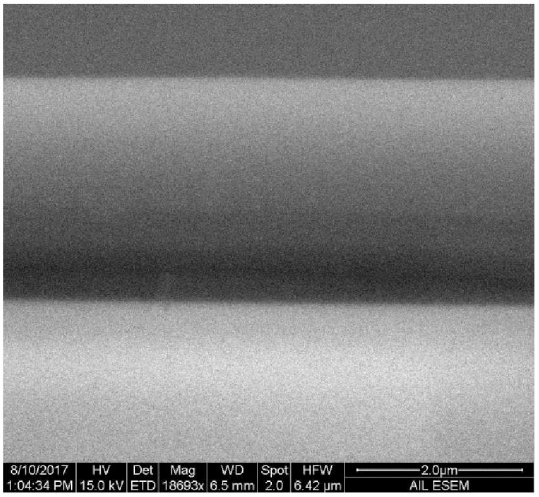

(d)

Figure 7: SEM images of PS coatings with thickness of (a) 1.7, (b) 1.9, (c) 2.1 and (d) 2.75 µm, made at different spin coating speeds.

Chapter 6

Conclusions and Future Work

We have successfully fabricated coatings of TiO_2 nanoellipsoids with aspect ratios of 1 to 6 on AA-2024T3 Al alloy. Corrosion performance of the coated samples in salt solution was investigated by analyzing the SEM imaging and the quantitative data extracted from potentiodynamic polarization scans and electrochemical impedance spectroscopy. The results can be concluded as follows:

(1) TiO_2-coated Al samples showed lower corrosion rate and higher impedance values compared to the bare Al sample. The bare Al substrate surface became fully dark and deteriorated after 14-day immersion. TiO_2 coatings are effective on the corrosion protection of Al alloy in saline environment.

(2) The coated samples showed an increase in current density at around 7–21-day immersion with increasing the immersion time owing to the corrosion-generated defects and damage such as cracks and pitting holes. At 21-day immersion, the bare Al substrate showed a decrease in the current density, which may be due to the large amount of corrosion products formed on the surface acting as a barrier layer.

(3) Among the coated samples, TiO_2 AR6 coated samples showed relatively lower corrosion current density compared to other samples, indicating their better corrosion performance.

(4) PS-TiO_2 AR6 nanocomposite coating was fabricated, where the pores of TiO_2 AR6 coating were sealed by polystyrene. We expect that this PS-TiO_2 AR6 nanocomposite coating will show better corrosion performance than the TiO_2 AR6 coating.

We believe the coatings of TiO_2 nanoellipsoids will be useful to protect facilities from fast corrosion in a saline environment. Future work will be focused on the fabrication of PS-TiO_2

nanocomposite coatings and investigation on their corrosion performance in various corrosive media.

Acknowledgments

I would like to thank my advisor Dr. Lei Zhang at the University of Alaska Fairbanks (UAF) for her kind assistance and guidance throughout the project. I would like to thank Dr. Junqing Zhang for his guidance and help on nanoparticle synthesis, coating fabrication and corrosion tests. I would like to thank my committee Dr. Rorik Peterson and Dr. Daisy Huang for their guidance. This research work is supported by the NASA EPSCoR Program Cooperative Agreement Notice (CAN) (NNX16AT46A). I acknowledge the support of NASA. I would like to thank the department of mechanical engineering at UAF for proving me with the teaching assistantship. I would really like to thank Dr. Ken Severin at UAF for providing the assistance with Scanning Electron Microscope. I am really grateful to my family and friends for their support throughout my master degree program. In Last but not Least I am dedicating this Thesis to my WIFE for being with me always through all thick and thin.

References

1. USGS Mineral Summaries: https://minerals.usgs.gov/minerals/pubs/commodity/aluminum/
2. NASA Corrosion Technology Laboratory https://corrosion.ksc.nasa.gov/index.htm
3. NACE International https://www.nace.org/home.aspx
4. Zhang, Lei, et al. "Using shape anisotropy to toughen disordered nanoparticle assemblies." *ACS nano* 7.9 (2013): 8043-8050.
5. Lin, S., H. Shih, and F. Mansfeld. "Corrosion protection of aluminum alloys and metal matrix composites by polymer coatings." Corrosion science 33.9 (1992): 1331-1349.
6. Li, X., et al. "Corrosion protection properties of anodic oxide coatings on an Al–Si alloy." Surface and Coatings Technology 200.5-6 (2005): 1994-2000.
7. Radhakrishnan, S., et al. "Conducting polyaniline–nano-TiO2 composites for smart corrosion resistant coatings." Electrochimica Acta 54.4 (2009): 1249-1254.
8. Ilevbare, G. O., et al. "Inhibition of pitting corrosion on aluminum alloy 2024-T3: effect of soluble chromate additions vs chromate conversion coating." Corrosion 56.3 (2000): 227-242.
9. Shen, G. X., Y. C. Chen, and C. J. Lin. "Corrosion protection of 316 L stainless steel by a TiO2 nanoparticle coating prepared by sol–gel method." Thin Solid Films 489.1-2 (2005): 130-136.
10. Murugaraj, Pandiyan, David Mainwaring, and Nelson Mora-Huertas. "Dielectric enhancement in polymer-nanoparticle composites through interphase polarizability." Journal of applied physics 98.5 (2005): 054304.

11. Chandra, Alexander, et al. "Study of polystyrene/titanium dioxide nanocomposites via melt compounding for optical applications." Polymer Composites 28.2 (2007): 241-250.

12. Winey, Karen I., and Richard A. Vaia. "Polymer nanocomposites." MRS bulletin 32.4 (2007): 314-322.

13. Winey, Karen I., Takashi Kashiwagi, and Minfang Mu. "Improving electrical conductivity and thermal properties of polymers by the addition of carbon nanotubes as fillers." MRS Bulletin 32.4 (2007): 348-353.

14. Schadler, L. S., L. C. Brinson, and W. G. Sawyer. "Polymer nanocomposites: a small part of the story." JOM 59.3 (2007): 53-60.

15. Fendler, Janos H., ed. Nanoparticles and nanostructured films: preparation, characterization, and applications. John Wiley & Sons, 2008.